Journal of Electroceramics, 13, 117–120, 2004

Modelling the Deposition of High-*k* Dielectric Films by First Principles

SIMON D. ELLIOTT* & HENRY P. PINTO
NMRC, University College Cork, Lee Maltings, Prospect Row, Cork, Ireland

Submitted February 13, 2003; Revised November 26, 2003; Accepted January 22, 2004

Abstract. Considerable interest is focussed on high-*k* dielectrics as replacements for the gate oxide in future MOSFETs. Atomic Layer Deposition (ALD) is the method of choice to produce conformal thin films for the gate dielectric, but a deeper understanding of this method is needed for process optimisation. For ALD of alumina, we use first principles density functional (DFT) calculations to describe the surface intermediates and pathways of precursor adsorption/decomposition at the atomic scale, yielding quantitative reaction energetics. This reveals the intrinsic limits on ALD growth rate as a function of OH coverage.

Keywords: Atomic Layer Deposition, ab initio calculations, oxide surface, alumina, high-*k* dielectrics

1. Introduction

Atomic Layer Deposition (ALD) is a chemical vapour deposition technique, suitable for the slow and controlled growth of thin, conformal oxide films [1]. Gaseous precursors are admitted separately into the reactor in alternate pulses, chemisorbing individually onto the substrate, rather than reacting in the gas-phase. The reactor is purged with an inert gas between precursor pulses. Insulating layers of aluminium sesquioxide (alumina, Al_2O_3) are fabricated by ALD for electroluminescent flat-screen-displays [1], for node DRAM and for read/write thin film heads [2]. Despite its modest dielectric constant ($k \sim 9$), the large band gap of alumina and the quality of its interface to silicon has made it a candidate for MOSFET gate dielectrics [3], possibly in combination with higher-*k* oxides. Successful precursors for alumina ALD are trimethylaluminium ($AlMe_3$, where $Me = CH_3$) and water (H_2O), which react to give solid alumina and methane:

$$AlMe_{3(g)} + 3/2 \cdot H_2O_{(g)} \rightarrow 1/2 \cdot Al_2O_{3(s)} + 3CH_{4(g)} \quad (1)$$

*To whom all correspondence should be addressed. E-mail: simon.elliott@nmrc.ucc.ie

Various models for the mechanism of alumina ALD have been proposed [4–6] but definitive evidence for the surface intermediates is lacking. We therefore use density functional theory (DFT) to investigate the atomic-scale structure and reactivity of hydroxylated and methylated alumina surfaces. The resulting mechanism allows us to establish the intrinsic limits to ALD growth. A previous DFT study of alumina ALD considered the energetics of $AlMe_3$ hydrolysis, including activation energies, under the unhindered conditions of a cluster model, rather than at a realistic surface [7]. Another presented an OH-terminated surface as the saturating step in alumina ALD [4].

2. Computational Method and Model

The First Principles method is established as a reliable way to predict bulk materials and surfaces [8]. Self-consistent DFT within 3D-periodic boundary conditions is used to compute the ground state electronic structure. We employ the VASP package [9–11] and use a standard set of technical parameters.[1] Amorphous alumina films are deposited by ALD [1], but this method is restricted to simulating periodic systems. As the most thermodynamically stable and best-characterised alumina polymorph, crystalline α-Al_2O_3

is chosen as the oxide substrate, terminated by the (0 0 0 1) basal plane. The surface is modelled by an infinite series of stacked slabs, separated by vacuum. Validation of this model[2] was reported previously [15]. This alumina surface is selected as the substrate (rather than Si, say), so as to simulate the later 'steady-state' stage of oxide-on-oxide ALD.

3. Results and Discussion

3.1. Hydroxylated Surface

A central question in the mechanism of the alumina ALD reaction (1) is the degree of hydroxylation of the substrate at the end of the H_2O pulse. Dissociative adsorption of H_2O from the ambient should ensure an OH-rich, saturated surface. On the other hand, H is lost via the reaction with surface Me and subsequent desorption as CH_4. We therefore consider two extremes: the bare Al_2O_3 surface, **1**, and a gibbsite-like $Al(OH)_3$ termination, **2** [4, 16]. The DFT-optimised surfaces are illustrated in Fig. 1. Under conditions of excess $H_2O_{(g)}$ and neglecting entropy effects [15], the hydroxylated surface **2** shows a much lower surface free energy ($\Delta G_{surf} = -2.2$ eV/$(1 \times 1) = -1.8$ J/m^2) and is therefore favoured.

Entropic contributions to the free energy will increase with temperature: above some temperature T_{crit}, H_2O desorption will dominate and the bare surface **1** will be favoured. To estimate T_{crit}, we calculate the translational entropy of an ideal gas of H_2O at a typical ALD pressure (3 Pa [5]) using the Sackur-Tetrode equation [17]. At $T_{crit} = 570 \pm 25$ K we find that $\Delta S = 366 \pm 12$ J·K^{-1}·mol^{-1}, so that $3/2 \cdot T_{crit} \Delta S$ equals the entropy-free ΔG_{surf} quoted above.[3] In $AlMe_3/H_2O$ ALD experiments, the growth rate is found to be highest over the broad temperature range 450–600 K [2, 5, 6, 18], with the drop in rate >600 K attributed to decreasing OH concentration. Our crude estimate of T_{crit} agrees remarkably closely with these findings and indicates that **2** is the appropriate model of reactive substrate for $AlMe_3$ adsorption (Section 3.2).

Clearly, the actual hydroxylated surface will not be as simple as the extreme cases presented here. Our DFT calculations reveal a wide range of adsorption and dissociation energies for H_2O on alumina (not presented here). At ALD temperatures of 450–600 K it is likely that a situation between **1** and **2** will occur, such as an AlO(OH) surface resembling bulk boehmite or diaspore. Alternatively, under high H_2O partial pressures, hydroxyl groups may penetrate many layers into the substrate [4, 16], giving a higher H concentration than **2**; the slowly saturating 'tail' of the H_2O pulse observed in ALD experiments supports this [18]. Such possibilities are therefore included in Table 1.

3.2. Adsorption of Trimethylaluminium

Based on the analysis in Section 3.1 above, the H_2O ALD pulse is found to produce a fully hydroxylated surface, **2**. Adsorption onto this substrate is therefore examined in order to simulate the $AlMe_3$ pulse. Adsorption is found to be a Lewis acid-base process and so barrier-free in the correct orientation: electrons are donated from the O of surface hydroxyl to the Al centre of the gas-phase precursor (**3**, Fig. 2). The adsorption energy ($\Delta E = -0.9$ eV/$AlMe_3 = -90$ kJ/mol) includes contributions from formation of a weak Al─O bond and from associated tilting of the surface OH. This relatively low ΔE means that desorption of $AlMe_3$ is expected to be facile at elevated temperatures.

Decomposition of the adsorbed precursor is possible during this pulse because of the high concentration of surface H in **2**. Our calculations show that bonding of

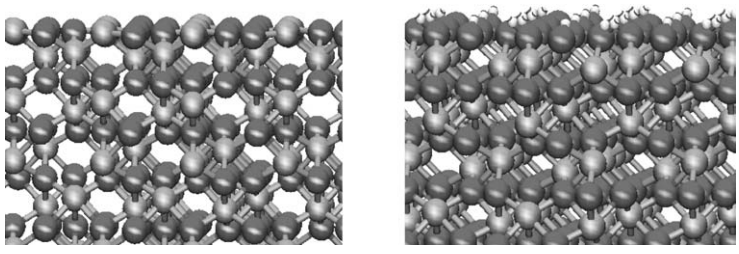

Fig. 1. Models for the alumina substrate at the end of the H_2O ALD pulse. (Ball-and-stick structural diagrams show non-physical "bonds" to guide the eye and balls for the atoms: large grey Al (light) and O (dark), medium C, and small H. [0 0 0 1] is vertical and a periodically repeating section of the surface is shown.) Left–**1**: Al_2O_3 bare (0 0 0 1) surface. Right - **2**: $Al(OH)_3$ model for hydroxylated surface.

Table 1. Limiting ALD rate for various degrees of saturating ("sat.") hydroxylation at the end of the H_2O pulse. The proportion of CH_4 to desorb ("des.") during each pulse is given. Surfaces are depicted in Fig. 1 (**1, 2**) and Fig. 2 (**5**).

H_2O pulse			$AlMe_3$ pulse			ALD rate	
Des. $CH_4 = 2/3x$	[H] sat.[a] $= 3x - 2$	Sat. surface	Des. $CH_4 = (3x-2)/3x$	[Al] sat.[a] $= x$	Sat. surface	$(Al_2O_3/\text{cycle}) = x/2$	(Å/cycle)[b]
100%	0	**1**: Al_2O_3	0%	2/3	**5**: Al_xMe_2	0.33	0.72
67%	1	AlO(OH)	33%	1	**5**: Al_xMe_2	0.50	1.08
40%	3	**2**: $Al(OH)_3$	60%	5/3	**5**: Al_xMe_2	0.83	1.80
29%	5	$Al(OH)_3.H_2O$	71%	7/3	**5**: Al_xMe_2	1.17	2.52

[a]Square brackets [X] indicate concentration of species X per (1×1) surface cell.
[b]The computed thickness of close-packed O layers of crystalline α-Al_2O_3 (2.16 Å) is used to obtain the rate in Å/cycle. Lower density amorphous layers are expected to be *ca.* 5% thicker.

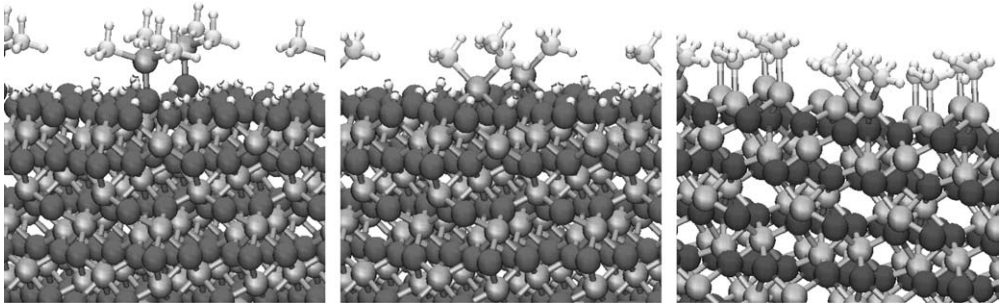

Fig. 2. Surface reactions during $AlMe_3$ ALD pulse. Left–3: $Al(Me)_3$ adsorbed on a hydroxylated substrate. Middle–decomposition by loss of CH_4 gives 4: $AlMe_2$. Right–Repeated adsorption and decomposition gives a saturated surface such as 5: Al_2Me_4 [15].

$AlMe_3$ to a surface OH makes this H more acidic, so that it can be transferred to adsorbate C, leading to CH_4 desorption and the release of -1.9 eV $= -180$ kJ/mol. The computed transition state (not shown) is at a C—H bond length of 1.7 Å and barrier of $E_a = +0.9$ eV relative to adsorbed $AlMe_3$, making the reaction thermally accessible at typical ALD temperatures. After this first decomposition step, the $AlMe_2$ remnant (**4**, Fig. 2) assumes a bridging position, between O and OH. In contrast to **3**, the exothermicity of decomposition means that **4** is more stable against desorption.

Depending on the kinetics of H diffusion along the surface, we suggest that further H transfer and decomposition will lead to AlMe groups. However the competing process of $AlMe_3$ adsorption/decomposition will proceed simultaneously and consume surface OH. Thus, a complex methylated surface will develop during the $AlMe_3$ pulse, which it is beyond the scope of our method to simulate. Instead, we assume that steric repulsion between Me groups is the limiting factor and find that the saturating concentration at the end of the pulse is about $2\text{Me}/(1\times1)$ or 17 μmol/m^2 [15], model **5** in Fig. 2. Surface models with higher Me concentration were found to be unstable. Optimised bond distances indicate that adsorbed Me are covalently bound and so are unlikely to desorb during the purge.

3.3. *Rate of ALD*

The models presented above do not reflect the dynamic complexity of the growing film during ALD. However the data motivate two assumptions: firstly, that all surface H and Me are sufficiently mobile to react completely to $CH_{4(g)}$ by the end of each pulse; and secondly, that full methylation results in the concentration $2\text{Me}/(1\times1)$ (Section 3.2). Then, considering the adsorption of a total of x molecules/cycle of $AlMe_3$ precursor onto a (1×1) surface cell, we rewrite reaction (1) as two half-reactions.

$$\text{AlMe}_3\text{ pulse: } (3x-2)\text{OH}_{(\text{surf})} + x(\text{AlMe}_3)_{(\text{g})} \rightarrow \text{Al}_\text{x}\text{Me}_{2(\text{surf})} + (3x-2)\text{CH}_{4(\text{g})} \quad (2)$$

$$\text{H}_2\text{O pulse: } \text{Al}_\text{x}\text{Me}_{2(\text{surf})} + 3x/2.(\text{H}_2\text{O})_{(\text{g})} \rightarrow (3x-2)\text{OH}_{(\text{surf})} + 2(\text{CH}_4)_{(\text{g})} \quad (3)$$

A full ALD cycle (2) + (3) results in deposition at the rate (x/2).Al_2O_3. The growth rate thus reflects the rate of Al adsorption, x. However, $AlMe_3$ adsorption is limited by Me concentration[4] (Section 3.2), and thus by CH_4 desorption during that pulse. While a total of $3x$ CH_4 molecules are desorbed per cycle, the proportion to be desorbed during either pulse is dictated by the H concentration. This is illustrated in Table 1 for some likely degrees of surface hydroxylation (from Section 3.1). For example, we predict a maximum rate of 1.8 Å/cycle for the **2**:$Al(OH)_3$ substrate.

A half monolayer/cycle growth rate is typically reported for this ALD reaction: 0.9–1.1 Å/cycle at 450–525 K, as measured by ellipsometry [2, 5] and quartz crystal microbalance (QCM) [6]. Quadrupole mass spectrometry shows about half of the CH_4 being desorbed during the $AlMe_3$ pulse [6], which matches our estimate for a moderately hydroxylated surface (between AlO(OH) and $Al(OH)_3$ in Table 1) and for a sub-monolayer limiting rate (1.08–1.80 Å/cycle). On the other hand, QCM weight changes of the same system indicate that 60–70% of the methane is lost during the $AlMe_3$ pulse [6], which according to our model (Table 1) corresponds to a more hydroxylated system and higher growth rate (1.80–2.52 Å/cycle). We stress that our calculated growth rates are ideal limiting values, based on perfect surfaces with no kinetics, so that these rates will not be attained in experiment. Even so, the calculated values are greatly in excess of experiment, which probably indicates that our estimate of saturating Me coverage is too high for these temperatures.

4. Conclusion

First Principles DFT calculations are used to elucidate the atomic-scale mechanism of alumina growth by Atomic Layer Deposition. Substantial surface hydroxylation is shown to result from H_2O exposure at typical ALD temperatures. The Al-containing precursor is found to adsorb weakly onto this surface, but decompose by H transfer to give a stable methyl overlayer. Combining these results yields a new picture of the ALD mechanism: a quantitative link between the amount of mobile surface H and the maximum growth rate, with results that are consistent with experiment.

Acknowledgments

We are grateful for funding by the European Community under the "Information Society Technologies" Programme through the HIKE project, http://www.nmrc.ie/hike, and acknowledge a generous grant of computing time from Photonics Theory, NMRC.

Notes

1. Technical parameters: plane-wave basis <396 eV, ultrasoft pseudopotentials [12], gradient-corrected density functional PW91 [13], sparse sampling of reciprocal space [14], self-consistent wavefunction converged to 10^{-4} eV, geometry optimisation (no symmetry restraints, no fixed atoms) to gradients $<10^{-3}$ eV/Å.
2. Slab parameters: 6 cation layers deep (13.1 Å), extended to (1×1) or (2×2) surface (30 or 120 atoms). Lattice parameters fixed at bulk and ionic coordinates relaxed fully; convergence for bare slabs of absolute energies <1 meV/Al_2O_3, interionic distances <0.04 Å, vacuum thicknesses >6 Å. Stoichiometric (singlet spin) systems with adsorbates on one side of the slab.
3. The factor 3/2 accounts for the 3/2.H_2O in the **2**:$Al(OH)_3$ (1×1) cell relative to **1**:Al_2O_3.
4. $AlMe_3$ adsorption will be limited by the number of surface Lewis base sites only at very high turnover, $x \sim 3$.

References

1. M. Leskelä and M. Ritala, *Thin Solid Films*, **409**, 138 (2002).
2. A. Paranjpe, S. Gopinath, T. Omstead, and R. Bubber, *J. Electrochem. Soc.*, **148,** G465 (2001).
3. E.P. Gusev, M. Copel, E. Cartier, I.J.R. Baumvol, C. Krug, and M.A. Gribelyuk, *Appl. Phys. Lett.*, **76**, 176 (2000).
4. R. Di Felice and J.E. Northrup, *Phys. Rev. B*, **60**, R16287 (1999).
5. A.W. Ott, J.W. Klaus, J.M. Johnson, and S.M. George, *Thin Solid Films*, **292**, 135 (1997).
6. A. Rahtu, T. Alaranta, and M. Ritala, *Langmuir*, **17**, 6506 (2001).
7. Y. Widjaja and C.B. Musgrave, *Appl. Phys. Lett.*, **80**, 3304 (2002).
8. M.J. Gillan, *J. Phys.: Condens. Matter*, **1**, 689 (1989).
9. G. Kresse and J. Hafner, *Phys. Rev. B*, **49**, 14251 (1994).
10. G. Kresse and J. Furthmüller, *Phys. Rev. B*, **54**, 11169 (1996).
11. G. Kresse and J. Furthmüller, *Comp. Mater. Sci.*, **6**, 15 (1996).
12. G. Kresse and J. Hafner, *J. Phys.: Condens. Matter*, **6**, 8245 (1994).
13. J.P. Perdew et al., *Phys. Rev. B*, **46**, 6671 (1992).
14. H.J. Monkhorst and J.D. Pack, *Phys. Rev. B*, **13**, 5188 (1976).
15. S.D. Elliott, *Electrochem. Soc. Proc. Vol.*, **231**, 2003 (2003).
16. C. Wolverton and K.C. Hass, *Phys. Rev. B*, **63**, 024102 (2001).
17. P.W. Atkins, *Physical Chemistry* (Oxford Univ. Press, Oxford, 1990).
18. R. Matero, A. Rahtu, M. Ritala, M. Leskelä, and T. Sajavaara, *Thin Solid Films*, **368**, 1 (2000).